Journal of Manufacturing Engineering, June 2023, Vol. 18, Issue. 2, pp 080-085

SIMULATION OF METALLIC WIRE-ARC ADDITIVE MANUFACTURING (WAAM) PROCESS USING SIMUFACT WELDING SOFTWARE

*** Vishal Kumar, Ankit Singh, Harish Bishwakarma and Amitava Mandal**

Department of Mechanical Engineering, Indian Institute of Technology (ISM) Dhanbad, Jharkhand -826004, India

ABSTRACT

Wire arc additive manufacturing (WAAM) is one of the emerging low-cost metal additive manufacturing techniques used to fabricate medium-large complex structures. The process provides design flexibility, supports green manufacturing, power efficiency, good structural integrity, high performance, and cost benefits, particularly for large-scale components. However, the heating and cooling cycle prevails during the deposition of material layer upon layer resulting in heat accumulation within the deposited layers. It causes geometric inaccuracy, surface roughness, high residual stresses, and mechanical anisotropy in the built structures. Therefore, SIMUFACT-Welding software has been used to model and simulate the WAAM process to fabricate a straight steel wall structure. The simulated results were able to visualize the existing thermal cycle during layer deposition and the effect of heat input on the fabricated wall structure and the substrate.

Keywords: *Metal additive manufacturing; WAAM; Simufact; Goldak heat source; Temperature profile; Weld bead*

1. Introduction

Direct energy deposition (DED) is a branch of metal additive manufacturing (AM) technologies that use metallic wire/powder as the feedstock material that fuses layer-upon-layer using a heat source such as a laser beam, plasma arc, electric arc, or electron beam [1]. Wire arc additive manufacturing (WAAM), a novel 'additive manufacturing' (AM) technique popular as DED-arc, is a production technique used to print 3D components or effectively repair metal parts. It has become a cost-effective option among other DED methods and a promising alternative to the traditional manufacturing technique in many aspects [2]. Compared to other additive manufacturing processes, WAAM techniques possess several other benefits, such as fabricating medium-to-large complex components, part design freedom, higher productivity, waste reduction, higher efficiency, equipment flexibility, and low start-up cost [3]. Based on the type of heat source used to melt the filler metallic wire, the WAAM technologies can be further classified into four groups: gas metal arc welding (GMAW-based WAAM), gas tungsten arc welding (GTAW-based WAAM), plasma arc welding (PAW-based WAAM) and cold metal transfer (CMT-WAAM) [4].

The technology is gaining utility in many industries, such as nuclear energy, aerospace (wing ribs and stiffened panels), automobile, marine (ship's propeller), and architecture (steel bridges) [5]. However, controlling the thermal cycle during the layer-upon-layer material deposition to fabricate the structure is still a significant challenge for this printing technique. The higher thermal gradients within the deposited layers are responsible for developing residual stresses, impart dimensional inaccuracy, surface roughness, and part distortion [6]. Through various experimental analyses and process simulations using ANSYS, ABAQUS, and COMSOL, the researchers attempted to closely monitor and control the heat transfer phenomena and thermal cycle during the WAAM-fabrication technique. To investigate the induced residual stresses and parts distortion in the fabricated WAAM component, Mughal et al. [7] developed a three-dimensional (3D) finite element (FE) model to predict part deformation and induced residual stress in the built component. The study observed unexpected deformation in the built part due to the complex thermal cycle that exists during layer deposition in the GMAW-based AM. The simulated results effectively cut off the number of trial experiments and thus save production time and cost associated with raw materials and energy losses.

Yong Ling et al. [8] conducted a series of thermo-mechanical analyses for the WAAM-built low-carbon steel component using the ABAQUS CEA software and artificial neural network (ANN)

**Corresponding Author - E- mail: vishal0101kumar@gmail.com*

methodology. The numerical investigation found good capability to predict the micro-hardness and tensile properties of the printed structure through the developed empirical model. In addition, Jiayi Zeng et al. [9] studied and established ideal models to examine the effect of heat input (HI) on the inter-layer bounding and surface quality of the wire arc additive manufactured straight wall structure using real-time thermal monitoring and 3D scanned data. The investigation observed a strong influence of heat input on the surface smoothness of the manufactured specimen and found that applying too high or too low heat input while depositing material deteriorates the surface quality and therefore is unfavourable. Furthermore, Seppala et al. [10] worked on the real-time surface temperature measurement during material deposition layer upon layer. The researcher observed infrared (IR) thermography as an excellent measurement of the existing temperature profile during AM. It is well accepted from previous studies that the surface quality and mechanical properties of the WAAM printed part largely depend on the thermal history during the part fabrication. Stavropoulos et al. [11] reviewed different thermo-mechanical modelling approaches for various AM processes. The investigation highlighted the importance of the HT model as it directly impacts the surface topography, mechanical strength, dimensional accuracy, and grain structure of the final fabricated structure. Most of the literature addresses process simulation using the finite element method using ABAQUS, ANSYS, and COMSOL multi-physics software. Modelling the thermal behaviour in the WAAM process is a complex step as it requires coupling three physical domains: mechanics, thermal, and metallurgy [12]. The SIMUFACT manufacturing software with a user-friendly FE simulation interface provides a simplified, purely mechanical solution.

Therefore, the study aims to explore the heat transfer phenomena during the WAAM process. Three layered wall structure built using the WAAM technique has been modelled using the MSC-Apex software, and simulated the fabrication process using the SIMUFACT-Welding software to visualize the existing temperature profile and the effect of the WAAM process parameter on the geometry of the built structure and substrate.

2. Materials Properties and Geometry

The WAAM technology comprises a welding machine such as MIG, TIG, or PAW setup integrated with a numerically controlled computer (CNC) table or robotic arm [13]. The configuration supply arc energy to melt and deposit metallic filler wire as the feedstock material. The welding nozzle attached to the robotic arm or CNC table provides flexibility in the deposition of material layer upon layer by controlling the deposition path and travel speed.

The Simufact Welding software simulated the WAAM process to deposit three-layer straight walls. The geometry used to simulate has been modelled in MSC Apex software and is shown in Fig. 1. The dimension of the base plate was taken as (300×300×5) mm^3, and that of single layer weld bead was (80×5×2) mm^3. The meshes of the transient three-layered wall structure modelled are shown in Fig. 2, and the detailed meshed structure parameters are illustrated in Table 1. The stainless steel (SS316) was used as the metallic filler wire and for the substrate over which wire was melted and deposited layer upon layer. The filler wire's material properties and elemental composition are shown in Fig. 3 and Table 2, respectively.

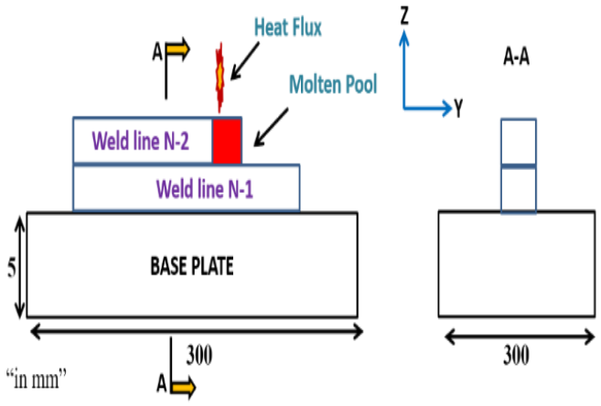

Fig. 1 Geometry used to simulate the WAAM process

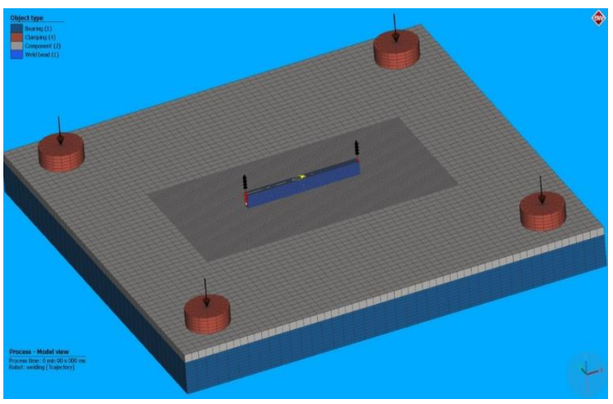

Fig. 2 The mesh of the transient model

Table 1 Detail of meshed WAAM structure

Geometry	Number of Nodes	Number of Elements
Wall Deposited	30107	25600
Substrate plate	64837	48960

Table 2 Elemental composition of metallic filler wire

Elements Wt.%	C	Cr	Mn	Mo	Ni	N	P	Si	Fe
Filler Wire	0.08	17.70	2.25	1.66	9.10	0.10	0.04	0.82	Bal.

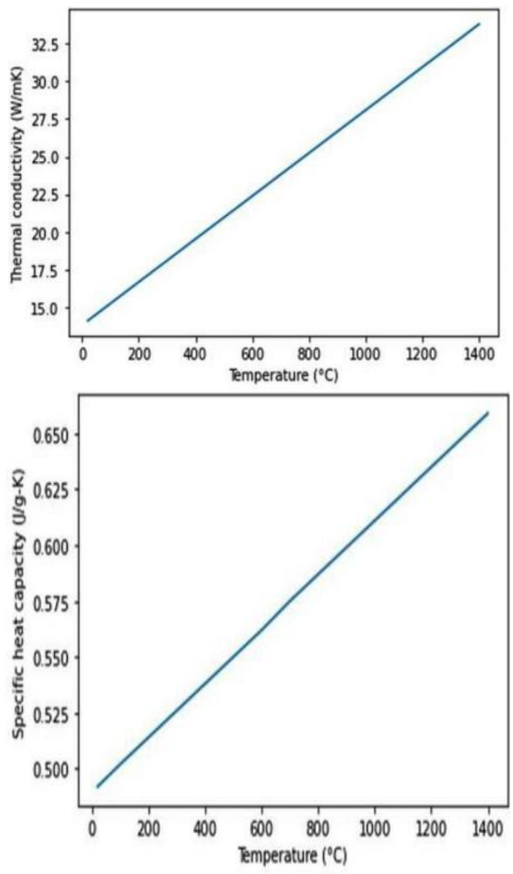

Fig. 3 Thermal properties of 316 SS (a) Thermal conductivity (b) Specific heat capacity

Table 3 WAAM Process parameter for layer deposition

S.No	Parameters	Ranges/Values
1.	Welding Voltage	18.5V
2.	Welding Current	120A
3.	Travel Speed	5.5 mm/sec
4.	Gross Energy	4036.36 J/cm

3. Heat Source Model

Goldak's heat source model with a double ellipsoidal heat profile has been applied to model the conventional welding heat source. The model follows a Gaussian heat distribution applied to the WAAM deposited bead. When moving along the feed direction (x-axis), the shape of the heat source model is determined by parameters like weld pool rear length (a_r), weld pool front length (a_f), weld pool depth (c) and width (b), as shown in Fig. 4. Similarly, the z-axis is oriented toward the arc aiming direction.

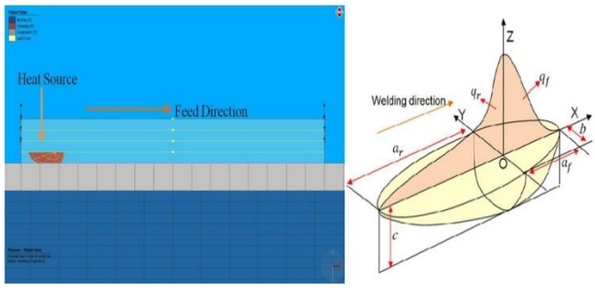

Fig. 4 Mesh element activation by moving heat source and Goldak's double ellipsoidal heat source model for heat flux distribution [14]

The power density of Goldak's heat source is specified via two volumetric heat flux rates as shown by equations (1) and (2), separately defined in the front region of the electric arc centre (Q_f) and region behind the arc centre (Q_r) respectively.

$$Q_f(x,y,z) = \frac{6\sqrt{3}\, f_f\, Q}{a_f bc\pi\sqrt{\pi}} exp(\frac{-3x^2}{a^2 f}) exp(\frac{-3y^2}{b^2}) exp(\frac{-3z^2}{c^2}) \quad (1)$$

$$Q_r(x,y,z) = \frac{6\sqrt{3}\, f_r\, Q}{a_r bc\pi\sqrt{\pi}} exp(\frac{-3x^2}{a^2 r}) exp(\frac{-3y^2}{b^2}) exp(\frac{-3z^2}{c^2}) \quad (2)$$

Coefficients b and c are the width and depth of the double ellipsoidal heat source model. Q is the heat input considering the factor of efficiency, and the magnitude is calculated by the equation of the applied power: $Q = \eta(VI)$, V and I are the open circuit voltage and welding current, and η is the process efficiency taken as 0.6. The detailed parameter values used in the simulation of the WAAM process have been shown in Table 4. The two dimensionless factors f_r and f_f are calculated by equations (3) and (4). It shows that the power density is distributed to the front and rear regions of the heat source model.

$$f_f = \frac{2}{(1+\frac{a_r}{a_f})} \quad (3)$$

$$f_r = \frac{2}{(1+\frac{a_r}{a_f})} \quad (4)$$

Table 4 Goldak's Heat source parameters

Parameters	a_r (mm)	a_f (mm)	b (mm)	c (mm)
Values	7.00	2.54	2.50	2.80

4. Results and Discussion

The temperature profile at three points of the first layer of the wall was recorded for the whole deposition of the three-layered wall structure in SIMUFACT-Welding software. Particle-1 and Particle-3 are placed at the surface of the start and end point of the first layer at the height of 1.5 mm, while Particle-2 is present at the same height but at the surface of the side of the wall. The recorded thermal cycle for the same is shown in Fig. 5, which shows the repetitive heating and cooling of the first layer during the deposition of each layer. The result shows that the maximum temperature achieved at Particle-2 is less than Particle-1 and Particle-3 for each layer deposition. This difference in maximum temperature exists because the Goldak heat source centre passes through Particle-1 and Particle-3 while Particle-2 coincides with the outer surface of the Goldak heat source. It is also visible from the obtained thermal profile that the temperature at different particles at the start of the deposition of the new layer increases with an increase in the number of layers.

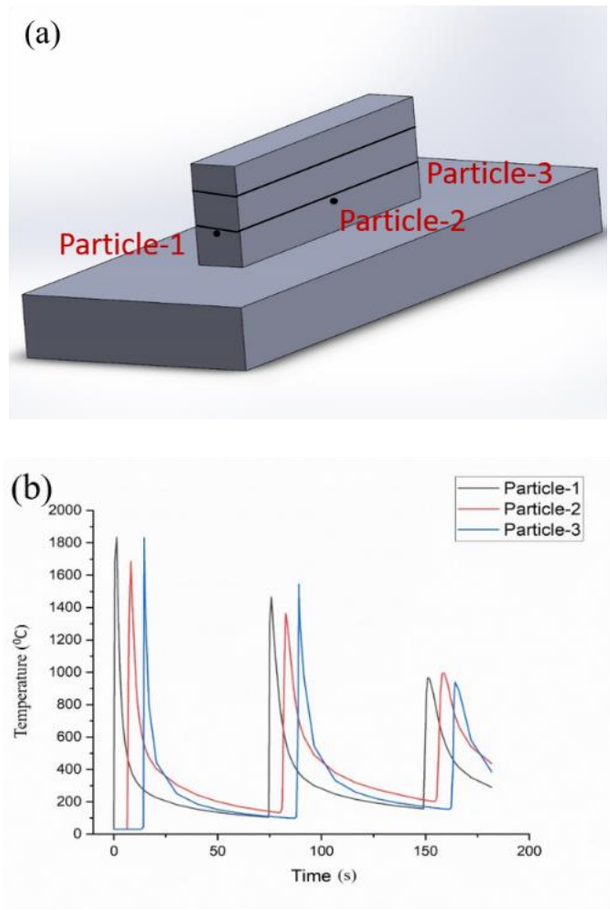

Fig. 5 Temperature profile at three distinct points on the first deposited layer while printing a three-layered WAAM structure

Thermal cycles were simultaneously measured at fixed spots on the substrates at their mid-lengths 10 mm, 15 mm, and 20mm off the deposition centerlines along the whole depositions, as shown in Fig. 6. The thermal cycle of the spots shows that the substrate had experienced repeated heating and cooling. The number of peaks obtained for each spot equals the number of layers deposited. There is a progressive increase in the temperature of each point due to the small inter-layer dwell time, which leads to the accumulation of heat with each new layer deposition. It means that we get a higher maximum temperature for each layer than the previous layer. The point selected from the deposited wall suffers less heat accumulation during part fabrication. The study would help to select optimal process parameters (inter-layer dwell time) and to decide the exact position of

clamps while printing WAAM components to mitigate distortion.

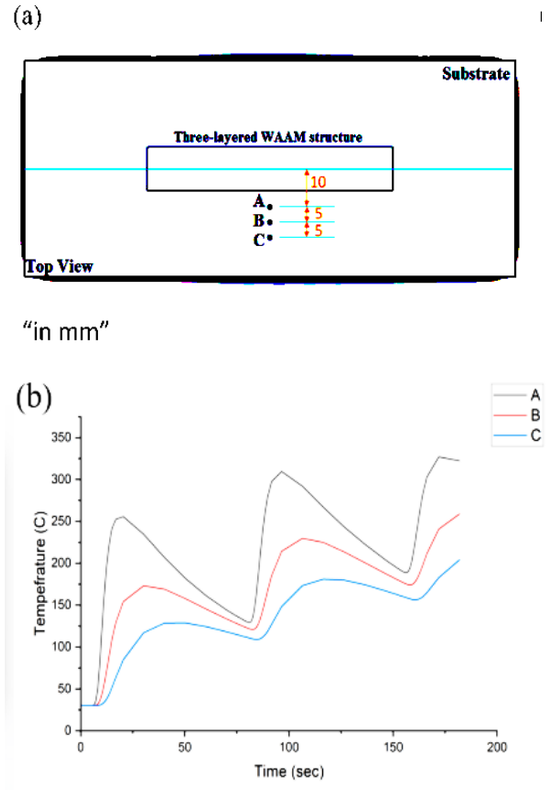

Fig. 6 Temperature profile at the selected particle on the substrate while printing a three-layered WAAM structure

5. Conclusions

In this research, SIMUFACT-Welding software has been used for modelling and simulating the WAAM process. Thermal cycles at various essential spots on the first deposited layer and the substrate are predicted through the simulation, and the following observations were obtained from the study:

i. The simulated results were able to visualize the existing thermal cycle during layer deposition and the effect of heat input on the fabricated wall structure and the substrate.

ii. Wall structure and substrate both experienced repeated heating and cooling during the deposition of material layer-upon-layer.

iii. The maximum temperature was obtained at the centre across the bead width direction and decreased along the width and minimum at both ends due to arcing phenomenon.

iv. Temperature decreases with increased distance from the deposition centerline due to heat convection from the deposited wall.

v. 4. There is a progressive increase in the temperature of spots on the substrate due to the heat accumulation that arises by using a short inter-layer dwell time that suggests the importance of dwell time while printing the WAAM part.

Acknowledgements

This work was supported by the Science and Engineering Research Board (DST-SERB), Govt. of India, under grant numbers [EEQ/2021/000l84].

Reference

1. *D. Svetlizky, et al., "Directed energy deposition (DED) additive manufacturing: Physical characteristics, defects, challenges and applications," Materials Today, vol. 49, pp. 271-295, 2021.*

2. *M. Belhadj, et al., "Thermal analysis of Wire Arc Additive Manufacturing process," 2021.*

3. *V. Kumar, et al., "Parametric study and characterization of wire arc additive manufactured steel structures," The International Journal of Advanced Manufacturing Technology, vol. 115, no. 5-6, pp. 1723-1733, 2021.*

4. *W. Jin, et al., "Wire arc additive manufacturing of stainless steels: a review," Applied Sciences, vol. 10, no. 5, p. 1563, 2020.*

5. *B. Wu, et al., "A review of the wire arc additive manufacturing of metals: properties, defects and quality improvement," Journal of Manufacturing Processes, vol. 35, pp. 127-139, 2018.*

6. *V. Kumar, B. K. Roy, and A. Mandal, "Thermal Modeling of Wire Arc Additive Manufacturing Process Using COMSOL Multiphysics," in Advances in Manufacturing Engineering: Select Proceedings of ICFAMMT 2022, Singapore: Springer Nature Singapore, 2022, pp. 223-232.*

7. *M. P. Mughal, H. Fawad, and R. A. Mufti, "Three-dimensional finite-element modelling of deformation in weld-based rapid prototyping," Proceedings of the Institution of Mechanical Engineers, Part C: Journal of Mechanical Engineering Science, vol. 220, no. 6, pp. 875-885, 2006.*

8. *Y. Ling, et al., "Numerical prediction of microstructure and hardness for low carbon steel wire Arc additive manufacturing components," Simulation Modelling Practice and Theory, vol. 122, p. 102664, 2023.*

9. *J. Zeng, W. Nie, and X. Li, "The influence of heat input on the surface quality of wire and arc additive manufacturing," Applied Sciences, vol. 11, no. 21, p. 10201, 2021.*

10. *J. E. Seppala and K. D. Migler, "Infrared thermography of welding zones produced by polymer extrusion additive manufacturing," Additive Manufacturing, vol. 12, pp. 71-76, 2016.*

11. *P. Stavropoulos and P. Foteinopoulos, "Modelling of additive manufacturing processes: a review and classification," Manufacturing Review, vol. 5, p. 2, 2018.*

12. *J.-M. Bergheau, "Modélisation numérique des procédés de soudage," Techniques de l'ingénieur. Génie mécanique BM7758, 2004.*

13. *V. Kumar, D. R. Sahu, and A. Mandal, "Parametric study and optimization of GMAW based AM process for Multi-layer bead deposition," Materials Today: Proceedings, vol. 62, pp. 255-261, 2022.*

14. *] Z. Samad, N. M. Nor, and E. R. I. Fauzi, "Thermo-Mechanical Simulation of Temperature Distribution and Prediction of Heat-Affected Zone Size in MIG Welding Process on Aluminium Alloy EN AW 6082-T6," IOP Conference Series: Materials Science and Engineering, vol. 530, no. 1, IOP Publishing, 2019.*